Supplementary material to the paper "Multiparticle correlations in complex scattering: birthday paradox and Hong-Ou-Mandel profiles in mesoscopic systems"

INTRODUCTION

The statistical study of quantum correlations due to indistinguishability in MB mesoscopic scattering can be carried out in two different, complementary ways. The powerful random matrix theory techniques introduced in Sec. II are suitable to address the universal regime where Hong-Ou-Mandel (HOM) effects can be neglected, namely, when the incoming wavepackets are mathematically taken as plane waves without a well defined position. Within random matrix theory, therefore, the effect of finite dwell time in the HOM profile is by definition irrelevant. In order to study the emergence of universality due to chaotic scattering on HOM profiles and the quantum-classical transition due to effective distinguishability, in Sec. III a semiclassical theory is implemented. The semiclassical approach is able to account for the effect of localized, shifted incoming wavepackets in the universal limit where only pairwise correlations are relevant, as shown in Sec. IV. Finally, in Sec, I the profile of the mesoscopic HOM effect is explicitly calculated.

I. CALCULATION OF THE GENERALIZED OVERLAP INTEGRALS $\mathcal{Q}^2(z)$

Using the definition Eq. (4), the amplitudes given in Eq.(3) and the correlator in Eq. (9) of the main text, we get

$$\mathcal{Q}^{(2)}(z) = \int_{E_\chi}^{\infty} dE_1 dE_2 \frac{\mathrm{e}^{i(q_2-q_1)z}}{1+\left[\frac{\tau_d(E_1-E_2)}{\hbar}\right]^2} \times \frac{m^2}{4\pi^2\hbar^2}\frac{|\tilde{X}(k-q_1)|^2|\tilde{X}(k-q_2)|^2}{\hbar^2 q_1 q_2}\,. \tag{1}$$

To further proceed, we use $E_i = E_\chi + \hbar^2 q_i^2/2m$ and $q = q_2 - q_1, Q = (q_1+q_2)/2$. Then we observe that in the momentum representation the incoming wavepackets $\tilde{X}(q_i - k)$ are strongly localized around $q_1 = q_2 = k$. As long as $ks \gg 1$ we can extend the lower limit of the integrals to $-\infty$ and keep only terms of first order in q. Under these conditions Eq. (1) yields

$$\mathcal{Q}^{(2)}(z) = \int_{-\infty}^{\infty} dQ dq \frac{\mathrm{e}^{iqz}}{1+v^2\tau_d^2 q^2} \times \frac{|\tilde{X}(Q-k-q/2)|^2|\tilde{X}(Q-k+q/2)|^2}{4\pi^2}\,, \tag{2}$$

which can be finally transformed into

$$\mathcal{Q}^{(2)}(z) = \int_{-\infty}^{\infty} \mathcal{F}^2(z-vt)\frac{\mathrm{e}^{-\frac{|t|}{\tau_d}}}{2\tau_d}dt\,. \tag{3}$$

II. RMT APPROACH FOR TRANSMISSION PROBABILITIES

In this section we derive and then prove results for the transmission probabilities of bosons and fermions in both symmetry classes, Eq. (13) in the main text.

A. Bosons

For n bosons, we start with the expression

$$\tilde{A}_n^+ = \frac{1}{\sqrt{n!}}\sum_{\mathcal{P}\in S_n}\prod_{k=1}^{n} Z_{i_k,o_{\mathcal{P}(k)}}\,, \tag{4}$$

where we sum over all permutations $\mathcal{P}$ of $\{1,\dots,n\}$ and where $Z = \sigma^{\mathrm{T}}$ is the transpose of the single particle scattering matrix σ (so we can identify the first subscript as an incoming channel and the second as an outgoing one). For simplicity we assume that all the channels are distinct. This quantity is related to the n-particle amplitude when the particle energies coincide or $\tau_d = 0$.

For the transmission probability we are interested in

$$|\tilde{A}_n^+|^2 = \tilde{A}_n^+(\tilde{A}_n^+)^* = \frac{1}{n!}\sum_{\mathcal{P},\mathcal{P}'\in S_n}\prod_{k=1}^{n} Z_{i_k,o_{\mathcal{P}(k)}}Z^*_{i_k,o_{\mathcal{P}'(k)}}\,. \tag{5}$$

The averages over scattering matrix elements are known both semiclassically and from RMT (see [1, 2] for example)

$$\left\langle Z_{a_1,b_1}\cdots Z_{a_n,b_n}Z^*_{\alpha_1,\beta_1}\cdots Z^*_{\alpha_n,\beta_n}\right\rangle = \sum_{\sigma,\pi\in S_n} V_N(\sigma^{-1}\pi)\prod_{k=1}^{n}\delta(a_k-\alpha_{\sigma(k)})\delta(b_{\bar{k}}-\beta_{\pi(\bar{k})})\,, \tag{6}$$

where V are class coefficients which can be calculated recursively.

However, since the channels are distinct, for each pair of permutations $\mathcal{P},\mathcal{P}'$ in Eq. (5) only the term with $\sigma = id$ and $\pi = \mathcal{P}(\mathcal{P}')^{-1}$ in Eq. (6) contributes. One then obtains the result

$$\tilde{P}_n^+ = \langle|\tilde{A}_n^+|^2\rangle = \frac{1}{n!}\sum_{\mathcal{P},\mathcal{P}'\in S_n} V_N(\tau)\,, \tag{7}$$

where

$$\tilde{P}_n^+ = \frac{1}{n!}\left\langle P^+_{\mathbf{a},\mathbf{b}}\right\rangle\Big|_{z_{ij}=0}^{\frac{\tau_d}{\tau_s}=0} \tag{8}$$

is the transmission probability when the particles enter at equal energies at the same time. In Eq. (7) $\tau = \mathcal{P}(\mathcal{P}')^{-1}$

is the target permutation of the scattering matrix correlator. Since τ is a product of two permutations, summing over the pair $\mathcal{P}, \mathcal{P}'$ just means that τ covers the space of permutations $n!$ times and

$$\tilde{P}_n^+ = \sum_{\tau \in S_n} V_N(\tau)\,. \tag{9}$$

Since the class coefficients only depend on the cycle type of τ, one could rewrite the sum in terms of partitions. For this we let $\boldsymbol{v}$ be a vector whose elements v_l count the number of cycles of length l in τ so that $\sum_l l v_l = n$. Accounting for the number of ways to arrange the n elements in cycles, one can write the correlator as

$$\tilde{P}_n^+ = \sum_{\boldsymbol{v}}^{\sum_l l v_l = n} \frac{n! V_N(\boldsymbol{v})}{\prod_l l^{v_l} v_l!}\,, \tag{10}$$

where we represent the argument of V by the cycles encoded in $\boldsymbol{v}$.

Typically, one considers correlators with a fixed target permutation, rather than sums over correlators as here in Eq. (9). For example fixing $\tau = (1, \ldots, n)$ provides the linear transport moments while $\tau = id$ gives the moments of the conductance. A summary of some of the transport quantities which have been treated with RMT and semiclassics can be found in [3].

1. Examples

Representing the argument of the class coefficients V_N instead by its cycle type, one can directly write down the result for $n = 1, 2$:

$$\begin{aligned} \tilde{P}_1^+ &= V_N(1) \\ \tilde{P}_2^+ &= V_N(1,1) + V_N(2)\,, \end{aligned} \tag{11}$$

while for $n = 3$ there are 6 permutations

$$\begin{array}{lll} (1)(2)(3) & (123) & (132) \\ (1)(23) & (12)(3) & (13)(2)\,, \end{array} \tag{12}$$

and so

$$\tilde{P}_3^+ = V_N(1,1,1) + 3V_N(2,1) + 2V_N(3)\,. \tag{13}$$

With the recursive results in [1, 2] for the class coefficients we can easily find the following results for low n:

2. Unitary case

Without time reversal symmetry, the results are

$$\begin{aligned} \tilde{P}_1^+ &= \frac{1}{N} \\ \tilde{P}_2^+ &= \frac{1}{N(N+1)} \\ \tilde{P}_3^+ &= \frac{1}{N(N+1)(N+2)} \\ \tilde{P}_4^+ &= \frac{1}{N(N+1)(N+2)(N+3)} \\ \tilde{P}_5^+ &= \frac{1}{N(N+1)(N+2)(N+3)(N+4)}\,. \end{aligned} \tag{14}$$

The pattern

$$\tilde{P}_n^+ = \frac{\Gamma(N)}{\Gamma(N+n)}\,. \tag{15}$$

holds for all n as we prove in a following subsection. In fact we can relate $n!\tilde{P}_n^+$ to the moments of a single element of a CUE random matrix and find a proof of Eq. (15) in [4].

For a comparison to diagrammatic results, the expansion in N^{-1} is

$$\tilde{P}_n^+ = \frac{1}{N^n} - \frac{n(n-1)}{2N^{n+1}} + \ldots \tag{16}$$

3. Orthogonal case

With time reversal symmetry, the results are

$$\begin{aligned} \tilde{P}_1^+ &= \frac{1}{(N+1)} \\ \tilde{P}_2^+ &= \frac{1}{N(N+3)} \\ \tilde{P}_3^+ &= \frac{1}{N(N+1)(N+5)} \\ \tilde{P}_4^+ &= \frac{1}{N(N+1)(N+2)(N+7)} \\ \tilde{P}_5^+ &= \frac{1}{N(N+1)(N+2)(N+3)(N+9)}\,, \end{aligned} \tag{17}$$

with a general result of

$$\tilde{P}_n^+ = \frac{\Gamma(N)}{\Gamma(N+n)} \frac{(N+n-1)}{(N+2n-1)}\,, \tag{18}$$

and an expansion of

$$\tilde{P}_n^+ = \frac{1}{N^n} - \frac{n(n+1)}{2N^{n+1}} + \ldots\,. \tag{19}$$

For a proof of Eq. (18) we can show that $n!\tilde{P}_n^+$ coincides exactly with the moments of a single element of a COE random matrix. The result as proved in [5] leads directly to Eq. (18).

B. Fermions

For n fermions we start instead with

$$\tilde{A}_n^- = \frac{1}{\sqrt{n!}} \sum_{\mathcal{P}\in S_n} (-1)^{\mathcal{P}} \prod_{k=1}^{n} Z_{i_k, o_{\mathcal{P}(k)}}\,, \tag{20}$$

where $(-1)^{\mathcal{P}}$ represents the sign of the permutation, counting a factor of -1 for each even length cycle in $\mathcal{P}$. Following the same steps for bosons, one has

$$\tilde{P}_n^- = \langle |\tilde{A}_n^-|^2 \rangle = \sum_{\tau\in S_n} (-1)^{\tau} V_N(\tau)\,, \tag{21}$$

so for example

$$\tilde{P}_3^- = V_N(1,1,1) - 3V_N(2,1) + 2V_N(3)\,. \tag{22}$$

Calculating the class coefficients recursively one then finds the following results for low n:

1. Unitary case

Without time reversal symmetry, the results are

$$\begin{aligned}
\tilde{P}_1^- &= \frac{1}{N} \\
\tilde{P}_2^- &= \frac{1}{N(N-1)} \\
\tilde{P}_3^- &= \frac{1}{N(N-1)(N-2)} \\
\tilde{P}_4^- &= \frac{1}{N(N-1)(N-2)(N-3)} \\
\tilde{P}_5^- &= \frac{1}{N(N-1)(N-2)(N-3)(N-4)}\,,
\end{aligned} \tag{23}$$

The pattern turns out to be

$$\tilde{P}_n^- = \frac{\Gamma(N-n+1)}{\Gamma(N+1)}\,, \tag{24}$$

and the expansion in N^{-1} is

$$\tilde{P}_n^- = \frac{1}{N^n} + \frac{n(n-1)}{2N^{n+1}} + \dots \tag{25}$$

2. Orthogonal case

With time reversal symmetry, the results are

$$\begin{aligned}
\tilde{P}_1^- &= \frac{1}{(N+1)} \\
\tilde{P}_2^- &= \frac{1}{(N+1)N} \\
\tilde{P}_3^- &= \frac{1}{(N+1)N(N-1)} \\
\tilde{P}_4^- &= \frac{1}{(N+1)N(N-1)(N-2)} \\
\tilde{P}_5^- &= \frac{1}{(N+1)N(N-1)(N-2)(N-3)}
\end{aligned} \tag{26}$$

with a general result of

$$\tilde{P}_n^- = \frac{\Gamma(N-n+2)}{\Gamma(N+2)} \tag{27}$$

and an expansion of

$$\tilde{P}_n^+ = \frac{1}{N^n} + \frac{n(n-3)}{2N^{n+1}} + \dots \tag{28}$$

C. Proofs

Now we can turn to proving the formulae in Eq. (24) and Eq. (27). These proofs build heavily on [5, 6] for the underlying details and methods. To introduce the techniques though, we start with the simpler case of reproving Eq. (15).

1. Unitary bosons

Starting with the sum over permutations in Eq. (9), we use the fact that the class coefficients, which are also known as the unitary Weingarten functions admit the following expansion [6]

$$\tilde{P}_n^+ = \sum_{\tau\in S_n} V_N(\tau) = \frac{1}{n!} \sum_{\lambda\vdash n} \frac{f^\lambda}{C_\lambda(N)} \sum_{\sigma\in S_n} \chi^\lambda(\sigma)\,, \tag{29}$$

where λ is a partition of n and the remaining term are as defined in [6]. To evaluate the sum we employ the character theory for symmetric groups. The trivial character for S_n is $\chi^{(n)}(\sigma) = 1$ for $\sigma \in S_n$ while the orthogonality of irreducible characters means that

$$\frac{1}{n!} \sum_{\sigma\in S_n} \chi^\lambda(\sigma)\chi^\mu(\sigma) = \delta_{\lambda,\mu}\,. \tag{30}$$

Combining both these facts we have

$$\frac{1}{n!} \sum_{\sigma\in S_n} 1\chi^\lambda(\sigma) = \sum_{\sigma\in S_n} \chi^{(n)}(\sigma)\chi^\lambda(\sigma) = \delta_{(n),\lambda}\,. \tag{31}$$

Substituting into Eq. (29) the gives

$$\tilde{P}_n^+ = \frac{1}{n!} \sum_{\lambda\vdash n} \frac{f^\lambda}{C_\lambda(N)} \delta_{(n),\lambda} = \frac{f^{(n)}}{C_{(n)}(N)}\,. \tag{32}$$

Since $f^{(n)} = 1$ and $C_{(n)}(N) = N(N+1)\dots(N+n-1)$ from the definitions in [6] we obtain

$$\tilde{P}_n^+ = \frac{1}{N(N+1)\dots(N+n-1)}\,, \tag{33}$$

recovering and proving Eq. (15).

2. Unitary fermions

For fermions we need to include the powers of (-1) in Eq. (21). For this we proceed as in the bosonic case, but now we for the powers of (-1) we use the irreducible character $\chi^{(1^n)}(\sigma) = (-1)^\sigma$ for $\sigma \in S_n$. Substituting into Eq. (21) gives

$$\tilde{P}_n^- = \frac{1}{n!}\sum_{\lambda\vdash n}\frac{f^\lambda}{C_\lambda(N)}\sum_{\sigma\in S_n}\chi^{(1^n)}(\sigma)\chi^\lambda(\sigma)\,, \tag{34}$$

while orthogonality reduces the result to

$$\tilde{P}_n^- = \frac{1}{n!}\sum_{\lambda\vdash n}\frac{f^\lambda}{C_\lambda(N)}\delta_{(1^n),\lambda} = \frac{f^{(1^n)}}{C_{(1^n)}(N)}\,. \tag{35}$$

Taking $f^{(1^n)} = 1$ and $C_{(1^n)}(N) = N(N-1)\dots(N-n+1)$ from the definitions in [6] we obtain

$$\tilde{P}_n^- = \frac{1}{N(N-1)\dots(N-n+1)}\,, \tag{36}$$

proving Eq. (24).

3. Orthogonal fermions

This proof is somewhat more involved and we start by expressing our sum

$$\begin{aligned}\tilde{P}_n^- &= \sum_{\tau\in S_n}(-1)^\tau V_N(\tau)\\ &= \sum_{\mu\vdash n}\frac{n!}{z_\mu}(-1)^{n-l(\mu)}\mathrm{Wg}^{\mathrm{O}}(\mu;N+1)\,,\end{aligned} \tag{37}$$

in terms of Wg^{O} which are the Weingarten function for the COE and which are evaluated for permutations τ of coset-type μ while z_μ is as defined in [5]. As in [5] we can reexpress our sum in terms of double length permutations

$$\tilde{P}_n^- = \frac{1}{2^n n!}\sum_{\sigma\in S_{2n}}\left(-\frac{1}{2}\right)^{n-l'(\sigma)}\mathrm{Wg}^{\mathrm{O}}(\sigma;N+1)\,, \tag{38}$$

where $l'(\sigma)$ is the length of μ if μ is the coset-type of σ. From the definition of the orthogonal Weingarten function [6] our sum becomes

$$\tilde{P}_n^- = \frac{1}{(2n)!}\sum_{\lambda\vdash n}\frac{f^{2\lambda}}{D_\lambda(N+1)}\sum_{\sigma\in S_{2n}}\left(-\frac{1}{2}\right)^{n-l'(\sigma)}\omega^\lambda(\sigma)\,, \tag{39}$$

in terms of zonal spherical functions ω^λ. These play the role of the irreducible characters used for the unitary case, and analogously as for the unitary fermions

$$\omega^{(1^n)}(\sigma) = \left(-\frac{1}{2}\right)^{n-l'(\sigma)}\,. \tag{40}$$

The zonal functions also follow an othogonality relation

$$\frac{1}{(2n)!}\sum_{\sigma\in S_{2n}}\omega^\lambda(\sigma)\omega^\mu(\sigma) = \frac{\delta_{\lambda,\mu}}{f^{2\lambda}}\,, \tag{41}$$

so that

$$\tilde{P}_n^- = \sum_{\lambda\vdash n}\frac{f^{2\lambda}}{D_\lambda(N+1)}\frac{\delta_{\lambda,(1^n)}}{f^{2\lambda}} = \frac{1}{D_{(1^n)}(N+1)}\,. \tag{42}$$

Finally from the definition of $D_\lambda(N+1)$ in [6] one has $D_{(1^n)}(N+1) = \prod_{i=1}^n(N+1-i)$ giving

$$\tilde{P}_n^- = \frac{1}{(N+1)N\dots(N-n+2)}\,, \tag{43}$$

proving Eq. (27).

D. Coinciding channels

We start with letting k outgoing channels (say b_i, $i = 1,\dots,k$) be identical while keeping the remaining outgoing channels and the incoming channels distinct. Then still only $\sigma = id$ is permissible in Eq. (6) while π can now take any value $\mathcal{K}\mathcal{P}$ for all $\mathcal{K}\in S_k$. The sum becomes

$$\hat{P}_n^\pm = \sum_{\mathcal{P}\in S_n}(\pm1)^{\mathcal{P}}\sum_{\mathcal{K}\in S_k}V_N(\mathcal{K}\mathcal{P})\,. \tag{44}$$

For each $\mathcal{K}$ we set $\tau = \mathcal{K}\mathcal{P}$ then since

$$(\pm1)^{\mathcal{P}} = (\pm1)^{\mathcal{K}^{-1}\tau} = (\pm1)^{\mathcal{K}^{-1}}(\pm1)^\tau = (\pm1)^{\mathcal{K}}(\pm1)^\tau\,, \tag{45}$$

the sum reduces to

$$\hat{P}_n^\pm = \sum_{\mathcal{K}\in S_k}(\pm1)^{\mathcal{K}}\sum_{\tau\in S_n}(\pm1)^\tau V_N(\tau)\,. \tag{46}$$

Since we already know the sum over τ

$$\hat{P}_n^\pm = \sum_{\mathcal{K}\in S_k}(\pm1)^{\mathcal{K}}\tilde{P}_n^\pm\,, \tag{47}$$

we are left with the simple sum over $\mathcal{K}$. For bosons, this is simply $k!$ while for fermions we can again use the irreducible characters and their orthogonality

$$\sum_{\mathcal{K}\in S_k}(-1)^{\mathcal{K}} = \sum_{\mathcal{K}\in S_k}\chi^{(1^k)}(\mathcal{K})\chi^{(k)}(\mathcal{K}) = k!\delta^{(1^k),(k)} = \delta_{k,1}\,, \tag{48}$$

since clearly (1^k) and (k) can only be the same partition when $k = 1$. Combined we have

$$\hat{P}_n^\pm = k!(1\pm1)\tilde{P}_n^\pm \qquad k>1\,. \tag{49}$$

We can repeat this process for arbitrary sets of coinciding incoming and outgoing channels giving the result for bosons that $\hat{P}_n^+ = \mathbf{a}!\mathbf{b}!\tilde{P}_n^+$ and zero for fermions as soon

as any channels coincide. For the unitary case there is no restriction on whether **a** or **b** contain the same channels, but in the orthogonal case as soon as this happens the simple formula in Eq. (6) is no longer valid and must be replaced by a more complicated version (see [1, 2] for example). With this restriction, these results provide Eq. (13) in the main text.

III. SEMICLASSICAL TREATMENT OF SCATTERING MATRIX CORRELATORS

We will treat correlators of A_n using a semiclassical diagrammatic approach. This is heavily based on [2, 3, 7, 8] and we refer in particular to [2, 7] for the underlying details and methods.

We return first to the transmission probability for bosons in Eq. (9). For a given cycle $(1, \ldots, l)$ in the target permutation τ the semiclassical trajectories have a very particular structure whereby we first travel along a trajectory with positive action from i_1 to o_1 and then in reverse back along a trajectory with negative action to i_2 and so on along a cycle until we return to i_1. For example for $n = 3$ we have the trajectory connections in Fig. 1(a) for each target permutation τ in Eq. (12).

For the actions of the diagram to nearly cancel, and to obtain a semiclassical contribution, the trajectories must be nearly identical, except at small regions called encounters. By directly collapsing the trajectories onto each other, as in Fig. 1(b) we obtain some of the leading order diagrams for each τ. In fact for each diagram, following the rules of [9], the semiclassical contribution is a factor of $-N$ for each encounter and a factor of N^{-1} for each link between the encounters. For each cycle of length l in the diagrams in Fig. 1(b) one then has a factor of order N^{-2l+1}.

As a straightforward example we can look at the simplest diagrams made up of a set of independent links like the first diagram in Fig. 1(b). With n links each providing the factor N^{-1} we have the contribution

$$\tilde{P}^{\pm} = N^{-n} \tag{50}$$

This contribution is in fact unaffected by the energy and time differences of the incoming particles leading directly to the classical contribution presented in Eq. (7) of the main text. This contribution also accounts for the leading order terms in the expansions of Eqs. (16), (19), (25) and (28).

A. Diagrammatic treatment without time reversal symmetry

Once the contribution of each diagram has been established, one then needs to generate all permissible diagrams. As shown in [2, 8] however the vast majority of semiclassical transport diagrams cancel. Those which remain can be untied until their target permutation becomes identity. For systems without time reversal symmetry, which we consider first, they can be mapped to primitive factorisations. One can reverse the process to build the diagrams by starting with a set of n independent links and tying together two outgoing channels into a new encounter. This tying process increases the order of the diagram by N^{-1}. If the outgoing channels are labelled by j and k then the target permutation also changes to $\tau(j\,k)$. For example going from the top left diagram of Fig. 1(b) tying together any two outgoing channels leads to the three example along the bottom row. The diagrams correspondingly move from order N^{-3} to N^{-4}.

Tying the remaining outgoing channel to one of those already tied leads to a diagram of the type further along the top row of Fig. 1(b) [for each of which there are 3 possible arrangements, and an alternative with a single larger encounter] and now of order N^{-5}.

Of course one could retie the same pair chosen in the first step, so that the target permutation is again identity. Such a diagram is however not shown in Fig. 1(b) but can be thought of as a higher order correction to a diagonal pair of trajectories. These types of diagrams appear when one treats the conductance variance for example. Such diagrams have a graphical interpretation which we will discuss below and use to generate them.

1. Forests

At leading order for each cycle of length l in τ the trajectories however form a ribbon graph in the shape of a tree. The tree has $2l$ leaves (vertices of degree 1) and all further vertices of even degree greater than 2. Such trees can be generated [10] by first treating unrooted trees whose contributions we store in the generating function f. Using the notation in [7], the function satisfies

$$f = \frac{r}{N} - \sum_{k=2}^{\infty} f^{2k-1}\,, \qquad \frac{f}{N} = \frac{\sqrt{1+\frac{4r^2}{N^2}}-1}{2r}\,, \tag{51}$$

where the power of r counts the number of leaves and the encounters may not touch the leads since the channels are distinct. Rooting the tree we add a leave to arrive at the generating function $F = rf$ while setting $r^2 = s$ we arrive at

$$\frac{F}{N} = \frac{\sqrt{1+\frac{4s}{N^2}}-1}{2}\,. \tag{52}$$

Expanding in powers of s

$$F = \frac{s}{N} - \frac{s^2}{N^3} + \frac{2s^3}{N^5} - \frac{5s^4}{N^7} + \frac{14s^5}{N^9} + \ldots \tag{53}$$

one has an alternating sequence of Catalan numbers, A000108 [11].

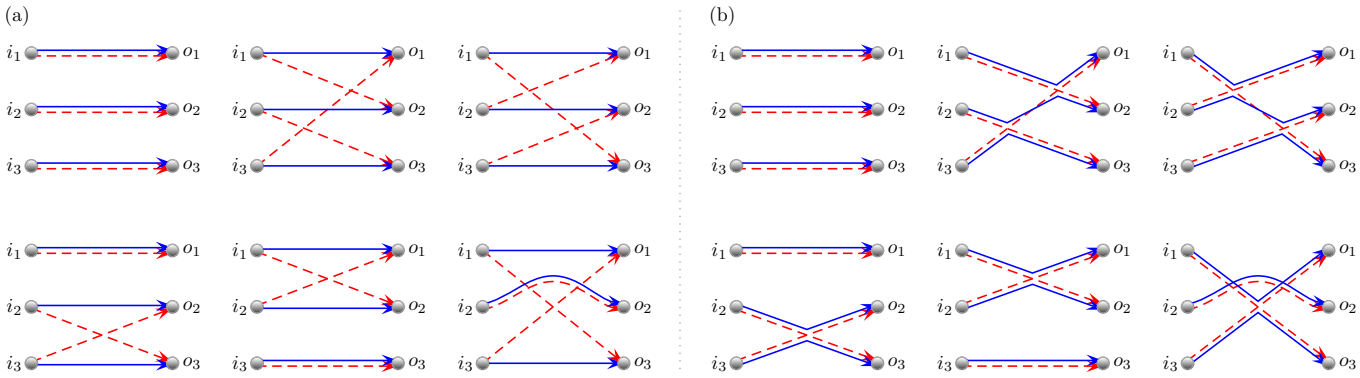

FIG. 1. (a) The permutations on 3 labels represented as trajectory diagrams. (b) Semiclassical contributions come when the trajectories are nearly identical, as when collapsed onto each other.

When summing over all permutations for τ, each cycle of length l can be arranged in $(l-1)!$ ways and we now wish to include this factor in the ordinary generating function. First we divide instead by a factor l with the transformation

$$\frac{K_0}{N} = \int \frac{F}{sN}\,\mathrm{d}s = \sqrt{1+\frac{4s}{N^2}} - 1 + \frac{1}{2}\ln\left[\frac{N^4\left(1-\sqrt{1+\frac{4s}{N^2}}\right)}{2s^2} + \frac{N^2}{s}\right], \tag{54}$$

so that K_0 becomes the exponential generating function of the leading order trees multiplied by the factor $(l-1)!$ as required. To now generate any forest of trees corresponding to all permutations τ we can exponentiate K_0 to obtain the exponential generating function

$$\mathrm{e}^{K_0} - 1 = \frac{s}{N} + \frac{(N-1)s^2}{2N^3} + \frac{(N^2-3N+4)s^3}{6N^5} + \frac{(N^3-6N^2+19N-30)s^4}{24N^7} + \ldots \tag{55}$$

whose first few terms can be explicitly checked against diagrams.

2. *Higher order corrections to trees*

For each given cycle $(1,\ldots,l)$ of τ there are higher order (in N^{-1}) corrections which can be organised in a diagrammatic expansion [3, 7]. For systems without time reversal symmetry, the first correction occurs two orders lower than leading order and the corresponding diagrams can be generated by grafting the unrooted trees on two particular base diagrams. Repeating the steps in [7], while excluding the possibility for encounters to touch the leads (since the channels are distinct), one first obtains

$$K_2 = -\frac{(f^2+3)f^4}{6(f^2+1)^3}, \tag{56}$$

where handily, the method for subleading corrections automatically undercounts by a factor of l so we directly obtain the required exponential generating function. Finally we substitute from Eq. (51) and find

$$12NK_2 = \frac{1+\frac{6s}{N^2}}{\left(1+\frac{4s}{N^2}\right)^{\frac{3}{2}}} - 1\,. \tag{57}$$

The exponential generating function $\mathrm{e}^{K_0+K_2}-1$ would then generate all corresponding diagram sets up to this order.

3. *Other corrections*

However, the higher order corrections to trees are less important than the higher order corrections to other target permutation structures. For any pair of cycles $(1,\ldots,k)(k+1,\ldots,l)$ in τ we can have diagrams which are order N^{-2} smaller than a pair of leading order trees. For example, tying any two outgoing channels of a tree on the cycle $(1,\ldots,l)$ would break the target permutation into two as here.

To generate diagrams with two cycles, we graft trees around both sides of a circle as for the cross correlation of transport moments treated in [7]. This will include the example with $n=3$ mentioned at the start of this subsection.

Following the steps in [7], while excluding the possibility of encounters touching the lead, one finds the generating function

$$\kappa = -\ln\left[\frac{1-f_1^2f_2^2}{(1-f_1^2)^2(1-f_2^2)^2}\right] + \ln\left[\frac{1}{(1-f_1^2)^2}\right] + \ln\left[\frac{1}{(1-f_2^2)^2}\right], \tag{58}$$

where f_1 and f_2 are the f in Eq. (51) but with arguments r_1 and r_2 respectively. The last two terms are corrections for when either r_1 or r_2 is 0 to remove diagrams with no

trees on either side of the circle. In [7], κ was differentiated and such terms removed automatically, but here this correction simplifies the result to

$$\kappa = -\ln\left[1 - f_1^2 f_2^2\right] . \tag{59}$$

This generating function again undercounts by both a factor of k and $(l-k)$ and can therefore be thought of as an exponential generating function of both arguments. Setting $s_1 = s_2 = s$ then sums the possible splittings of the l elements into two cycles (along with the combinatorial factor of choosing the label sets), counting each splitting twice. This then provides the following exponential generating function

$$\begin{aligned}\kappa_1 &= -\frac{1}{2}\ln\left[1 - f^4\right] \\ &= -\frac{1}{2}\ln\left[\frac{N^4}{2s^2}\left(\sqrt{1+\frac{4s}{N^2}}\left(1+\frac{2s}{N^2}\right) - 1 - \frac{4s}{N^2}\right)\right] ,\end{aligned} \tag{60}$$

whose expansion is

$$\kappa_1 = \frac{s^2}{2N^4} - \frac{2s^3}{N^6} + \frac{29s^4}{4N^8} - \frac{26s^5}{N^{10}} + \dots \tag{61}$$

4. Order of contributions

With the diagrams treated so far the exponential generating function would be

$$\begin{aligned}\mathrm{e}^{K_0+\kappa_1+K_2} - 1 = \frac{s}{N} &+ \frac{(N^3 - N^2 + N - 1)s^2}{2N^5} \\ &+ \frac{(N^4 - 3N^3 + 7N^2 - 15N + 20)s^3}{6N^7} \\ &+ \dots\end{aligned} \tag{62}$$

and the differences from Eq. (55) occur two orders lower in N^{-1} than the leading term from independent links. This is because the additional diagrams required at least two tying operations. However, we wish to know how the contributions change when n scales with N in some way.

First we can compare the contributions coming from K_2 to those from K_0. In the forest we can replace any tree from K_0 with its higher order correction in K_2. Since there can be at most n trees, and the correction is order N^{-2} smaller, these corrections will be bound by nN^{-2}, up to the scale of the generating function coefficients. This means that we can expect the contributions from K_2 to not be important when $n = o(N^2)$ as we take the limit $N \to \infty$.

Next we compare the contributions coming from κ_1 to those from K_0. In the forest we can now replace any tree by breaking its l cycle into two, say k and $(l-k)$. Alongside the generating function coefficients, the two new cycles come with the factor $(l-k-1)!(k-1)!$ instead of the $(l-1)!$ that was with the tree. Since

$$\begin{aligned}&\frac{1}{(l-1)!}\sum_{k=1} l - 1 \left(\begin{array}{c} l \\ k \end{array}\right)(l-k-1)!(k-1)! \\ &= \sum_{k=1}^{l-1} \frac{l}{(l-k)k} \leq l ,\end{aligned} \tag{63}$$

this contribution is bound by nN^{-1} and should not be important when $n = o(N)$.

Continuing in this vein we could break up any tree into three cycles and generate those diagrams but this should also be higher order when $n \ll N$. Keeping our expansion to this order we should have

$$\begin{aligned}\mathrm{e}^{K_0+\kappa_1} - 1 = \frac{s}{N} &+ \frac{(N^2 - N + 1)s^2}{2N^4} \\ &+ \frac{(N^3 - 3N^2 + 7N - 12)s^3}{6N^6} + \dots\end{aligned} \tag{64}$$

B. Time reversal symmetry

With time reversal symmetry, additional diagrams become possible. For example we may reverse the trajectories on one side of the circle used for cross correlations and obtain $2\kappa_1$ instead of just κ_1. There are also additional base diagrams at the second order correction to trees, which may be treated as in [7], but which we do not treat here since there are now diagrams at the the first order correction. These can be generated by grafting trees around a Möbius strip. Following again the steps in [7] while excluding the possibility of encounters touching the lead one obtains the generating function

$$K_1 = \frac{1}{2}\ln\left[\frac{1-f^2}{1+f^2}\right] , \tag{65}$$

or explicitly

$$\begin{aligned}K_1 &= -\frac{1}{4}\ln\left[1 + \frac{4s}{N^2}\right] \\ &= -\frac{s}{N^2} + \frac{2s^2}{N^4} - \frac{16s^2}{3N^6} + \frac{16s^4}{N^8} - \frac{256s^5}{5N^{10}} + \dots\end{aligned} \tag{66}$$

Compared to the leading order forest, we could replace any tree by its higher order correction and obtain a term bound by nN^{-1}, again up to the scale of the generating function coefficients. Restricting to $n = o(N)$ the the exponential generating function would be

$$\begin{aligned}\mathrm{e}^{K_0+2\kappa_1+K_1} - 1 = \frac{(N-1)s}{N^2} &+ \frac{(N^2 - 3N + 7)s^2}{2N^4} \\ &+ \frac{(N^3 - 6N^2 + 28N - 75)s^3}{6N^6} \\ &+ \dots\end{aligned} \tag{67}$$

C. Fermions

For fermions we need to also include the powers of (-1) in Eq. (21). However, because our semiclassical generating functions are organised by cycle type, we simply need to replace s by $-s$ and multiply the K type functions by -1 appropriately.

D. The variance

Now for n bosons we look at

$$|\tilde{A}_n^+|^4 = \frac{1}{(n!)^2} \sum_{\substack{\mathcal{P},\mathcal{P}' \\ \mathcal{R},\mathcal{R}' \in S_n}} \prod_{k=1}^{n} Z_{i_k,o_{\mathcal{P}(k)}} Z^*_{i_k,o_{\mathcal{P}'(k)}} \times Z_{i_k,o_{\mathcal{R}(k)}} Z^*_{i_k,o_{\mathcal{R}'(k)}} , \tag{68}$$

or rather the average

$$L_n^+ = \left\langle |\tilde{A}_n^+|^4 \right\rangle . \tag{69}$$

However, when we now compare to Eq. (6) such an average involves summing over permutations of length $2n$ while each of the originally distinct channels appears exactly twice. For example

$$L_1^+ = \langle Z_{i_1,o_1} Z_{i_1,o_1} Z^*_{i_1,o_1} Z^*_{i_1,o_1} \rangle = 2V_N(1,1) + 2V_N(2) , \tag{70}$$

since the delta function conditions in Eq. (6) are satisfied for any choice of σ and π. The result is

$$L_1^+ = \frac{2}{N(N+1)} \qquad L_1^+ = \frac{2}{N(N+3)} , \tag{71}$$

without or with time reversal symmetry respectively.

For $n = 2$, we can run through the sums of permutations, giving

$$L_2^+ = \frac{3N^2 - N + 2}{N^2(N^2-1)(N+2)(N+3)} , \tag{72}$$

without time reversal symmetry and

$$L_2^+ = \frac{3N^2 + 5N - 16}{N(N^2-4)(N+1)(N+3)(N+7)} , \tag{73}$$

with. For large n this process however quickly becomes computationally intractable. Diagrammatically, we can imagine multiplying the sets of diagrams we had before, but also keeping track of all the possible permutations and which channels coincide. For example we could take the diagrams in Fig. 1(b), add the remaining 5 copies of each diagram created by permuting the outgoing labels, and multiply the entire set by itself to obtain pairs of diagrams which appear for the variance. Of course each pair is over counted $(n!)^2$ times and we would still need to account for the diagrams where the pairs interact and where the repeated channels play a role by considering diagrams acting on $2n$ leaves.

To reduce the difficulty of such a diagrammatic expansion, we focus here instead on just calculating the leading order term. We know that these terms are represented diagrammatically by sets of independent links so we select the $(n!)^2$ such sets from our multiplication. Since each outgoing channel (although appearing twice) is distinct we may relabel them appropriately to reduce our leading order diagrams to $n!$ ways of permuting a single outgoing label. The sum of a product of two permutations essentially reduces to a sum over a single permutation. The overcounting is now $n!$ instead. For $n = 3$ the leading order diagrams are depicted in Fig. 2. For each diagram we have the standard leading order result of N^{-2n} which, when dividing by the over counting, would be the total result if the outgoing channels were different.

However, for each cycle of the effective permutation of the outgoing channels, an additional semiclassical diagram is possible. By adding a 2-encounter to each pair of identical channels we can separate them into two artificially distinct channels. The resulting semiclassical diagram can be drawn as a series of 2-encounters around a circle with one link on either side. This process is depicted in Fig. 3. The resulting starting point is from the larger set of possible trajectory correlators than just the sets of independent links squared, but once we move all the encounters into the appropriate leads, the required channels coincide and we have an additional leading order diagram.

To count such possibilities we just need to include a power of 2 for each cycle in the permutation of the outgoing channels when we include the standard diagonal terms. For each cycle of length l there are $(l-1)!$ different permutations so that

$$-2\log(1-s) = 2s + s^2 + \frac{2s^3}{3} + \frac{s^4}{2} + \dots \tag{74}$$

acts as the exponential generating function of both possibilities for each cycle times their number of permutations. To generate all leading order diagrams we simply exponentiate this function

$$\mathrm{e}^{-2\log(1-s)} - 1 = \frac{1}{(1-s)^2} - 1 \tag{75}$$

Since we are still overcounting by $n!$ this actually provides the ordinary generating function and when we include the semiclassical contributions of N^{-2n} we get the final leading order result of

$$L_n^+ = \frac{n+1}{N^{2n}} + o(N^{-2n+1}) \tag{76}$$

or a variance of

$$L_n^+ - \left(\tilde{P}_n^+\right)^2 = \frac{n}{N^{2n}} + o(N^{-2n+1}) \tag{77}$$

We checked this against the explicit semiclassical or RMT results involving Eq. (6) for n up to 5. Since the semiclassical diagrams all involve pairs of equally long cycles, the leading order result is also the same for fermions.

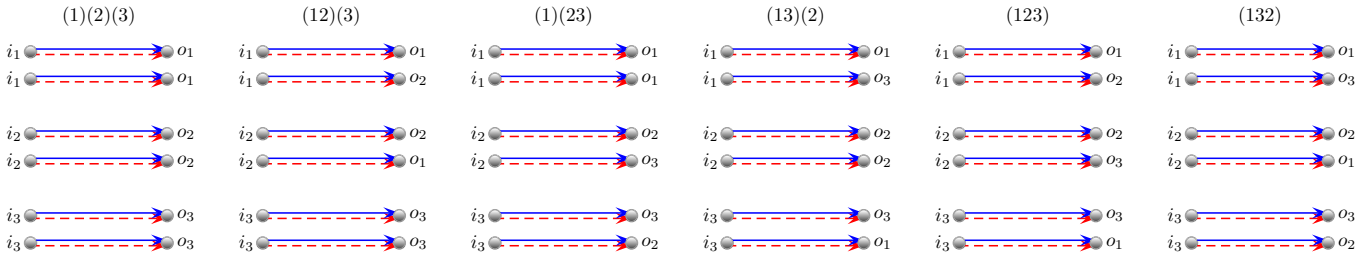

FIG. 2. The leading order diagrams for the variance with 3 particles are created by finding semiclassical diagrams with 6 incoming and outgoing channels. When the channels coincide, the leading order diagrams must reduce to separated links corresponding to one of the permutations on 3 labels depicted.

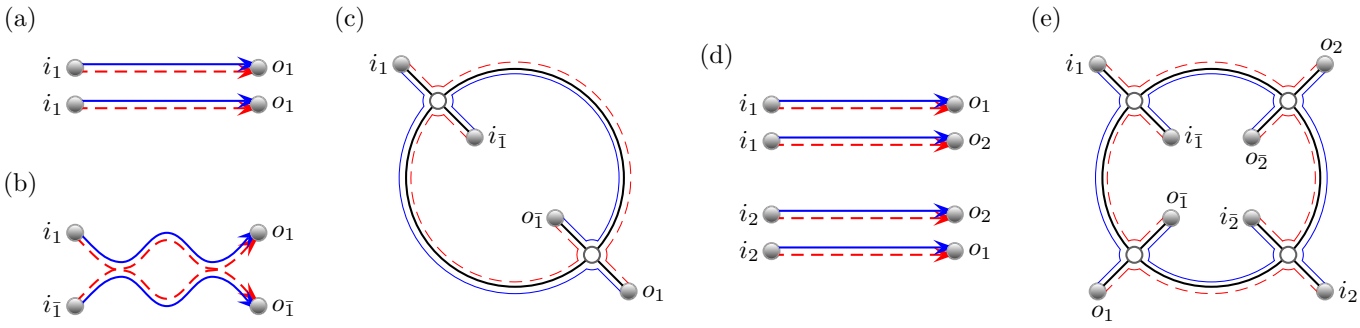

FIG. 3. (a) A pair of independent links can be joined by an encounter at each end to create the diagram in (b) with artificially distinct incoming and outgoing channels. When the encounters are moved into the incoming and outgoing leads respectively, the channels again coincide leading to a new leading order semiclassical diagram. In the graphical representation, the trajectories in (b) become the boundary walks around both sides of the circle in (c). Starting with four links corresponding to the permutation (12) in (d) we can create the correlated quadruplet represented in (e). Again moving the encounters into the leads creates a new leading order contribution.

Intriguingly, the numerator of the leading order result for the second moments in Eq. (76) is identical to the second moment of the modulus squared of the permanents of $n \times n$ random complex Gaussian matrices [12]. Higher moments of such permanents would be useful to determine the validity of the *Permanent Anti-Concentration Conjecture* important for Boson Sampling [12]. This opens the possibility that a semiclassical or RMT treatment of the higher moments of many body scattering, expanded just to leading order, could help answer such questions.

IV. RELEVANCE OF DIAGRAMS WITH PAIRWISE CORRELATIONS IN THE SCALING LIMIT

In the following sections we rigurously shown that in the limit $n \to \infty$ and under the scaling $N = \alpha n^2$ the sum of semiclassical diagrams with pairwise correlations gives Eq. (15) of the main text if $\tau_d/\tau_s = 0, z_{ij} = 0$. Once this result is stablished, we re-introduce $\tau_d/\tau_s > 0, z_{ij} \neq 0$ and obtain Eq. (16), one of our main results.

A. The case $\tau_d/\tau_s = 0, z_{ij} = 0$

In order to show that only diagrams with pairwise correlations are neccesary to obtain Eq. (15) in the main text, we start with the following exact relation

$$\frac{\langle P^{(\epsilon)}_{\mathbf{a},\underline{\mathbf{b}}}\rangle}{\langle P^{(\mathrm{cl})}_{\mathbf{a},\underline{\mathbf{b}}}\rangle}\bigg|^{\frac{\tau_d}{\tau_s}=0}_{z_{ij}=0} = \frac{\partial^n}{\partial s^n}\, \mathrm{e}^{K_0(s)}\Big|_{s=0} \tag{78}$$

expressing the ratio between quantum and classical transition probabilities in terms of the generating function $K_0(s)$ defined in Eq. (54). In the limit $n, N \to \infty$ with quadratic scaling $N = \alpha n^2$, all bounds in Sec. III A 4 show we only need to consider standard trees and forests. The generating function K_0 generates trees, with each power of s corresponding to trees with increasing number of leaves. Just s by itself is individual links, s^2 are the pairwise correlations, s^3 would be all three way correlator and so on. If we truncate to second order we only have links and x-like correlations in our generating function while further exponentiating K_0 truncated to second order generates all possible sets of links and pairwise correlators, like (a), (b), and (e) but not (d) in Fig. 2 of the main text.

Our strategy is to show that, in the scaling limit, Eq. (78) gives Eq. (15) of the main text when $K_0 =$

$s-s^2/2N+\mathcal{O}(s^3)$ is truncated to second order and therefore only pairwise correlations are included. Our starting point is then Eq. (78) with $K_0 = s(1-s/2N)$,

$$\frac{\langle P^{(\epsilon)}_{\mathbf{a},\underline{\mathbf{b}}}\rangle}{\langle P^{(\mathrm{cl})}_{\mathbf{a},\underline{\mathbf{b}}}\rangle}\bigg|^{\frac{\tau_d}{\tau_s}=0}_{z_{ij}=0} \simeq \frac{\partial^n}{\partial s^n}\,\mathrm{e}^{s\left(1-\frac{s}{2N}\right)}\Big|_{s=0}, \tag{79}$$

which can be written in the convenient form for asymptotic analysis

$$\begin{aligned}\frac{\partial^n}{\partial s^n}\,\mathrm{e}^{s\left(1-\frac{s}{2N}\right)}\Big|_{s=0} &= \frac{n!}{2\pi i}\oint \frac{\mathrm{e}^{z\left(1-\frac{z}{2N}\right)}}{z^{n+1}} \\ &= \frac{n!}{2\pi i}\oint \mathrm{e}^{z\left(1-\frac{z}{2N}\right)-(n+1)\log z}\end{aligned} \tag{80}$$

as a complex integral along a contour that enlcoses the origin. In the large n limit this integral can be evaluated in saddle point approximation. The saddle point $z = z^c$ is easily found to be

$$z^c = \frac{N}{2}\left(1-\sqrt{1-\frac{4(n+1)}{N}}\right) \simeq n+1+\frac{(n+1)^2}{N}. \tag{81}$$

The exponent in Eq. (80) and its second derivative evaluated at the saddle point are also easily found to be

$$\begin{aligned}&\left(z\left(1-\frac{z}{2N}\right)-(n+1)\log z\right)\Big|_{z=z^c} \simeq -(n+1)\log(n+1) \\ &+(n+1)-\frac{(n+1)^2}{2N}, \\ &\frac{\partial^2}{\partial z^2}\left(z\left(1-\frac{z}{2N}\right)-(n+1)\log z\right)\Big|_{z=z^c} \simeq \frac{1}{n+1}\end{aligned} \tag{82}$$

to get

$$\frac{\partial^n}{\partial s^n}\,\mathrm{e}^{s\left(1-\frac{s}{2N}\right)}\Big|_{s=0} \simeq \frac{n!}{2\pi}\frac{\sqrt{2\pi(n+1)}}{((n+1)/\mathrm{e})^{n+1}}\mathrm{e}^{-\frac{(n+1)^2}{2N}} \tag{83}$$

and finally, using the asymptotic approximation for the factorial of large numbers,

$$\frac{\partial^n}{\partial s^n}\,\mathrm{e}^{s\left(1-\frac{s}{2N}\right)}\Big|_{s=0} \simeq \mathrm{e}^{-\frac{n^2}{2N}}. \tag{84}$$

We conclude then that in the limit $n\to\infty$ and under the scaling $N=\alpha n^2$ the sum of semiclassical diagrams with pairwise correlations gives Eq. (15) of the main text.

B. The case $\tau_d/\tau_s > 0, z_{ij} \neq 0$

If only pairwise correlations are included in the diagramatic expansion, all results are expressed in terms of the overlapping functions between all posible pairs of incoming channels. This is a simple combinatorial problem and we get (for $\eta > 1$)

$$\frac{\langle P^{(\epsilon)}_{\mathbf{a},\mathbf{b}}\rangle}{\langle P^{(\mathrm{cl})}_{\mathbf{a},\mathbf{b}}\rangle} \xrightarrow[N=\alpha n^\eta]{n\gg 1} \sum_{\substack{\mathfrak{I}\subseteq\{1,\ldots,n\}\\ |\mathfrak{I}|=:2l \text{ even}}} \frac{(-\epsilon)^l}{N^l}\sum_{\mathcal{C}\sqcap\mathfrak{I}}\prod_{q=1}^{l}\mathcal{Q}^{(2)}(z_{\mathcal{C}_q}), \tag{85}$$

where $\mathcal{C}$ runs over the set of contractions obtained by pairing different indexes in $\mathfrak{I}=\{i_1,\ldots,i_{2l}\}$ and $\mathcal{C}_q$ is its qth element.

C. Mesoscopic HOM effect with two macroscopically occupied channels

In the following the explicit evaluation of Eq. (85) in the case of a very large number $n \gg 1$ of particles that macroscopically occupy only two different incoming wavepackets is carried out. Let $n_0 = y_0 n$ denote the number of particles in a single incoming wavepacket for which we set $z = 0$ and let $n_1 = y_1 n$ be the number of remaining particles occupying a wavepacket with separation $z = z_1$ from the other. We denote the corresponding sets of indexes with $\mathfrak{I}_0$ and $\mathfrak{I}_1$, respectively.

Pairings of the n particle indices are characterized by the total number of pairs l. Furthermore this number splits into the number l_1 of pairs among the n_0 indexes in $\mathfrak{I}_0$, the number k of pairs connecting an index in $\mathfrak{I}_0$ with one in $\mathfrak{I}_1$ and the number $l-l_1-k$ of pairs inside $\mathfrak{I}_1$. Each contraction specified by the numbers l, l_1, k contributes a value of

$$\left(\frac{-\epsilon}{N}\right)^l [\mathcal{Q}^{(2)}(0)]^{l-k}[\mathcal{Q}^{(2)}(z_1)]^k =: \left(\frac{-\epsilon}{\alpha}\right)^l n^{-2l} q_0^{l-k} q_1^k \tag{86}$$

to the sum in Eq. (85) if the scaling $N=\alpha n^2$ is taken into account. We introduced the abbreviations q_0 and q_1 for the two overlap integrals involved. Therefore the probability to get all particles in different outgoing channels is

$$\begin{aligned}\frac{\langle P^{(\epsilon)}_{\mathbf{a},\underline{\mathbf{b}}}\rangle}{\langle P^{(\mathrm{cl})}_{\mathbf{a},\underline{\mathbf{b}}}\rangle} \xrightarrow[N=\alpha n^2]{n\gg 1} &\sum_{l=0}^{\left[\frac{n}{2}\right]}\sum_{l_1=0}^{\min\left\{l,\left[\frac{n_1}{2}\right]\right\}}\sum_{k=0}^{\min\{l-l_1,n_1-2l_1\}} \\ &\times C_{l,l_1,k}\left(\frac{-\epsilon}{\alpha}\right)^l n^{-2l} q_0^{l-k} q_1^k,\end{aligned} \tag{87}$$

where the combinatorial factor for each tuple (l, l_1, k) is given by

$$\begin{aligned}C_{l,l_1,k} &= \underbrace{\binom{n_1}{2l_1}(2l_1-1)!!}_{l_1 \text{ pairs in } \mathfrak{I}_1}\ \underbrace{\binom{n_1-2l_1}{k}\binom{n_0}{k}k!}_{k \text{ pairs between } \mathfrak{I}_0 \text{ and } \mathfrak{I}_1} \\ &\times \underbrace{\binom{n_0-k}{2l-2l_1-2k}(2l-2l_1-2k-1)!!}_{\text{remaining pairs in } \mathfrak{I}_0} \\ &= \frac{1}{2^{l-k}l_1!(l-l_1)!}\binom{l-l_1}{k} \\ &\times \underbrace{\left[\frac{n_1!}{(n_1-2l_1-k)!}\frac{n_0!}{(n_0-2l+2l_1+k)!}\right]}_{\xrightarrow{n\gg 1} n_1^{2l_1+k}n_0^{2l-2l_1-k}}.\end{aligned} \tag{88}$$

The limiting value of the expression in square brackets is valid for any fixed l, l_1 and k. After expressing n_0 and n_1 by their (finite) fractions of n the addends of (87) become independent of n (due to the scaling $N = \alpha n^2$). This is the point where it becomes evident that a scaling of N with a power of n different from $\eta = 2$ would lead to trivial results corresponding to Eq. (15) of the main text (for $\eta > 1$) also in the present case where $\tau_d \neq 0$ and $z_{ij} \neq 0$ for some i, j. Simplifying the upper limits of the sums for $n \to \infty$ yields

$$\begin{aligned}\frac{\langle P^{(\epsilon)}_{\mathbf{a},\underline{\mathbf{b}}}\rangle}{\langle P^{(\mathrm{cl})}_{\mathbf{a},\underline{\mathbf{b}}}\rangle} &\xrightarrow[N=\alpha n^2]{n\gg 1} \sum_{l=0}^{\infty}\sum_{l_1=0}^{l}\frac{1}{l!}\left(\frac{-\epsilon}{2\alpha}\right)^l \binom{l}{l_1}\left(q_0 y_1^2\right)^{l_1} y_0^{l-l_1} \\ &\quad\times \sum_{k=0}^{l-l_1}\binom{l-l_1}{k}(q_0 y_0)^{l-l_1-k}(2q_1 y_1)^k \\ &= \sum_{l=0}^{\infty}\frac{1}{l!}\left(\frac{-\epsilon}{2\alpha}\right)^l \sum_{l_1=0}^{l}\binom{l}{l_1}\left(q_0 y_1^2\right)^{l_1}\left(2q_1 y_0 y_1 + q_0 y_0^2\right)^{l-l_1} \\ &= \sum_{l=0}^{\infty}\frac{1}{l!}\left(\frac{-\epsilon}{2\alpha}\right)^l \left(q_0\left(y_0^2+y_1^2\right)+2q_1 y_0 y_1\right)^l \\ &= \exp\left[-\frac{\epsilon}{4\alpha}\left(\mathcal{Q}^{(2)}(0)\left(1+x^2\right)+\mathcal{Q}^{(2)}(z_1)\left(1-x^2\right)\right)\right], \end{aligned} \tag{89}$$

where in the last step we rewrote q_0 and q_1 in terms of overlap functions and introduced the imbalance parameter x related to y_0 and y_1 by

$$\begin{aligned} y_0 &= \frac{1}{2}(1-x)\,, \\ y_1 &= \frac{1}{2}(1+x)\,. \end{aligned} \tag{90}$$

Equation (89) is plotted and analysed in Fig. 1 of the main text and corresponds to the result Eq. (16) there.

[1] P. W. Brouwer and C. W. J. Beenakker, *J. Math. Phys.* **37**, 4904- (1996).
[2] G. Berkolaiko and J. Kuipers, *J. Math. Phys.* **54**, 112103 (2013).
[3] G. Berkolaiko and J. Kuipers, *J. Math. Phys.* **54**, 123505 (2013).
[4] J. Novak, *E. J. Comb.* **14**, R21 (2007).
[5] S. Matsumoto, *Rand. Mat.: Theory Appl.* **1**, 1250005 (2012).
[6] S. Matsumoto, *Rand. Mat.: Theory Appl.* **2**, 1350001 (2013).
[7] G. Berkolaiko and J. Kuipers, *New J. Phys.* **13**, 063020 (2011).
[8] G. Berkolaiko and J. Kuipers, *Phys. Rev. E* **85**, 045201 (2012).
[9] S. Müller, S. Heusler, P. Braun, and F. Haake, *New J. Phys.* **9**, 12 (2007).
[10] G. Berkolaiko, J. M. Harrison, and M. Novaes, *J. Phys. A* **41**, 365102 (2008).
[11] N. J. A. Sloane, The on-line encyclopedia of integer sequences, published electronically at http://www.research.att.com/∼njas/sequences/
[12] S. Aaronson and A. Arkhipov, *Theory Comp.* **9**, 143- (2013).